TISSUE ENGINEERING: Part A
Volume 15, Number 4, 2009

DOI: 10.1089/ten.tea.2008.0092

Smooth Muscle Cell Seeding of Decellularized Scaffolds: The Importance of Bioreactor Preconditioning to Development of a More Native Architecture for Tissue-Engineered Blood Vessels

Saami K. Yazdani, Ph.D., Benjamin Watts, Masood Machingal, M.S., Yagna P.R. Jarajapu, Ph.D., Mark E. Van Dyke, Ph.D., and George J. Christ, Ph.D.

Vascular smooth muscle cells (VSMCs) impart important functional characteristics in the native artery and, therefore, should logically be incorporated in the development of tissue-engineered blood vessels. However, the native architecture and low porosity of naturally derived biomaterials (i.e., decellularized vessels) have impeded efforts to seed and incorporate a VSMC layer in tissue-engineered blood vessels. To this end, the goal of this study was to develop improved methods for seeding, proliferation, and maturation of VSMCs on decellularized porcine carotid arteries. Decellularized vessels were prepared in the absence and presence of the adventitial layer, and statically seeded with a pipette containing a suspension of rat aortic VSMCs. After cell seeding, recellularized engineered vessels were placed in a custom bioreactor system for 1–2 weeks to enhance cellular proliferation, alignment, and maturation. Initial attachment of VSMCs was dramatically enhanced by removing the adventitial layer of the decellularized porcine artery. Moreover, cyclic bioreactor conditioning (i.e., flow and pressure) resulted in increased VSMC proliferation and accelerated formation of a muscularized medial layer in the absence of the adventitial layer during the first week of preconditioning. Fura-2–based digital imaging microscopy revealed marked and reproducible depolarization-induced calcium mobilization after bioreactor preconditioning in the absence, but not in the presence, of the adventitia. The major finding of this investigation is that bioreactor preconditioning accelerates the formation of a significant muscular layer on decellularized scaffolds, in particular on adventitia-denuded scaffolds. Further, the VSMC layer of bioreactor-preconditioned vessels was capable of mobilizing calcium in response to cellular depolarization. These findings represent an important first step toward the development of tissue-engineered vascular grafts that more closely mimic native vasculature.

Introduction

Since the seminal work of Weinberg and Bell (1986),[1] the development of vascular substitutes has evolved from synthetic polymer conduits to nonthrombogenic scaffolds, such as endothelialized tubular scaffolds.[2,3] Although the presence of a confluent monolayer of endothelial cells (ECs) on the luminal surface has been shown to prolong the patency rates of implanted grafts in a variety of cardiovascular applications, the functional performance of these grafts over time still remains suboptimal compared to the native artery. A potential cause for the current deficiencies in bioengineered vascular grafts is the lack of medial smooth muscle cell (SMC) layer upon implantation. Vascular smooth muscle cells (VSMCs) comprise the vast majority of the cellular parenchyma of the medial layer of the vessel wall in native artery, and play an important role in vessel function throughout the vascular tree, assuming an ever more important role as vessel diameter narrows. In fact, VSMCs modulate vessel responses to a plethora of physiological stimuli, including mechanical and biochemical/pharmacological factors.[4] Moreover, synthetic grafts seeded with VSMCs have been shown to increase both EC retention and nitric oxide production *in vitro*.[5,6] Undeniably then, the presence of VSMCs would be expected to improve the functional characteristics of bioengineered vascular grafts.

In this regard, a number of studies have investigated VSMC seeding on synthetic and naturally derived vascular scaffolds. Yu *et al.*[5] studied methods for enhancement of VSMCs attachment on polytetrafluoroethylene (PTFE) grafts

Wake Forest Institute for Regenerative Medicine, Wake Forest University School of Medicine, Winston-Salem, North Carolina.

in vitro, and determined that seeding efficiency on PTFE was optimized in grafts precoated with fibronectin. Moreover, retention of ECs on the luminal surface was increased from 39% to 73% when ECs were seeded in combination with VSMCs *in vitro*. In a similar study, adhesion of VSMCs to polymer was enhanced by precoating synthetic scaffolds (poly-4-hydroxybutyrate) with an attachment solution containing collagen I, Matrigel, and gelatin to increase cell–matrix adhesion.[7] The attached VSMCs were confluent on the outer surface of the scaffold, with some penetration into the construct after 14 days of bioreactor preconditioning. No functional data for the seeded VSMCs were reported. Li *et al.*[8] observed that coating ePTFE vascular grafts with binding peptides increased attachment and proliferation of VSMCs. Niklason *et al.*[9] seeded VSMCs isolated from bovine aorta on polyglycolic acid scaffolds. In those studies, the surface of the polyglycolic acid scaffolds was chemically modified with sodium hydroxide, leading to improved VSMCs attachment. The seeded VSMCs reorganized and aligned on the outer layer of the vessel after 8 weeks of bioreactor preconditioning. Functional studies of these bioengineered vessels demonstrated contractile responses with a magnitude of $\approx$5% that of native arteries.

Despite these notable advancements, no engineered graft capable of normal vascular contractility has been developed *in vitro*. In that regard, current techniques to seed and precondition synthetic grafts have not yet been optimized to permit the VSMC attachment, proliferation, and migration required for formation of a physiologically relevant (i.e., contractile) medial SMC layer, although clear progress has been made.[10] While Badylak *et al.*[11] introduced the concept of using native collagen-rich matrices (small intestinal submucosa) as potential vascular grafts in 1989, the studies conducted to date have largely focused on ECs seeded grafts only. Although decellularized scaffolds possess many desirable characteristics (architecture, mechanical properties, and biochemical signals) for use as vascular replacements, they also have low porosity and are water tight, eliminating the possibility of direct injection of VSMCs into the vessel wall, thus impeding development of a medial SMC layer. McFetridge *et al.*[12] utilized three different techniques to seed acellular arteries with VSMCs and clearly documented the inability of VSMCs to penetrate beyond the adventitial–medial boundary. In another report,[13] 8 weeks of bioreactor conditioning appeared to achieve improved SMC integration/distribution into the wall of a decellularized porcine scaffold, but again, no functional measures were obtained.

In short, conventional approaches seem to have intrinsic limits that prevent formation of organized, multilayer VSMCs in decellularized arteries using bioreactor protocols, even after 8 weeks. Thus, no one has yet derived functional smooth muscle layers both on and within the wall of the construct, that is, bioengineered vessels with contractions that approximate native vascular responses *in vitro*. As a first step toward development of bioengineered vessels with a more physiologically relevant medial smooth muscle layer, our strategy in the present study was to use bioreactor preconditioning in combination with surface modification of decellularized vascular scaffolds to increase cellular seeding efficiency and proliferation, thus promoting a more uniform deposition and density of mature VSMCs in the engineered vessel. The overall goal of these experiments was to continue development/optimization of *in vitro* techniques for fabrication of tissue-engineered blood vessels with a more native vessel phenotype.

Materials and Methods

Cell culture

Primary cultures were established by harvesting VSMCs from the aorta of rats weighing approximately 600–700 g using an explant culture method according to a protocol approved by the Wake Forest University Animal Care and Use Committee. Briefly, the thoracic aorta was removed and placed in phosphate-buffered saline containing 1% antibiotics–antimitotics (Gibco, Grand Island, NY). The adventitia was carefully removed under a sterile hood by manual dissection, and the remaining vessel was cut into $\approx$1 mm^2 segments. The segments were positioned into six-well culture dishes and incubated in culture medium (Dulbecco's modified Eagle's medium containing low glucose, L-glutamine, 110 mg/L sodium pyruvate, pyridoxine hydrochloride [Gibco Life Technologies, Paisley, United Kingdom], 10% fetal bovine serum [Valley Biomedical, Winchester, United Kingdom], and 1% antibiotics–antimitotics). Cells migrated out of the tissue and adhered to the bottom of the culture dish. The VSMCs were maintained in a culture incubator at 37°C, 5% CO_2, and 95% relative humidity. The cells used for seeding experiments were between passages 2 and 5.

Decellularization process

Carotid arterial segments were obtained from large pigs (400–600 lb, Nifong Farm, Midway, NC). The blood vessels had an internal diameter of 3–4 mm and were cut into segments of approximately 50 mm in length. Vessels were washed in deionized (DI) water for 24 h and incubated in 0.05% Trypsin– ethylenediaminetetraacetic acid (GIBCO–Invitrogen, Carlsbad, CA) for 1 h. The vessels were incubated in decellularization solution (490 mL DI water, 10 mL Triton-100×, and 3.4 mL ammonium hydroxide) for 3 days in a mechanical rotating shaker at 4°C. The decellularization solution was changed daily. The decellularized vessels were then placed in DI water for an additional 48 h to wash away any residual processing chemicals from the matrix and then frozen for 24 h in a −80°C freezer, lyophilized (Labconco, Kansas City, MO), and sterilized with ethylene oxide. Hematoxylin and eosin (H&E) staining was performed to verify that all cellular components were removed from the matrix.

Adventitial removal

To remove the adventitia layer, the decellularized porcine carotid arterial segments were individually positioned onto an 18Fr balloon angioplasty catheter. Once inflated to 1 atm pressure, the internal diameters of the decellularized vessels were expanded to 6 mm. A dissecting stereo microscope (2.5×) was then used to make an incision to the subadventitia layer with a 15-gauge blade. At this stage, the adventitia could clearly be identified from the underlying media layer. A curved tip surgical tweezer was then used to gently strip off the adventitia layer from the media layer (see Fig. 4 for details). The entire procedure is quite simple and reproducible and takes $\approx$3–5 min to complete. The adventitia-free decellularized porcine arteries were then frozen, lyophilized, and sterilized with ethylene oxide. H&E staining was performed

to validate this structural modification, that is, the absence of the adventitia layer.

Static seeding

Before the bioreactor experiments, a series of static seeding experiments were performed to determine the optimal scaffold configuration and seeding density. More specifically, in a preliminary set of experiments scaffolds were seeded with a range of different cell densities (5×10^6 to 50×10^6 cells/mL); further, we explored different seeding orientations for the scaffold (data not shown). In short, the best conditions for static seeding of the scaffold were obtained by seeding 50×10^6 cells/mL while the scaffolds were submerged in the culture medium. For these experiments, scaffolds were first hydrated in the culture media for 4 h and cut into 4×4 mm square segments in a sterile manner under a culture hood. Using a hemostat clamp, the square segments were pinned using 26-gauge needles to individual wells of a 24-well culture dish. Careful consideration was taken to ensure that the intima layers of the square segments were pinned downward. Five hundred microliters of culture media was added to each well to ensure that the tissue pieces were completely submerged. Twenty microliters of VSMCs suspensions containing 50×10^6 cells/mL was then pipetted onto each segment in a consistent manner. At 1 day, 3 days, and 7 days after static seeding, individual recellularized segments were evaluated with H&E and DAPI staining.

Seeding and bioreactor conditioning

Before placement in the bioreactor system, the scaffolds were hydrated in culture media for 3 h and cut into rings of approximately 5 mm in length. The rings were placed on a custom-made elastomeric silicone tube (Sylgard 184; Dow Corning, Midland, MI) with 4 mm outer diameter and a 0.5 mm wall thickness. The tube was positioned into a bioreactor where the rings could be submerged in culture media before static seeding. Twenty microliters aliquots of a VSMC suspension (50×10^6 cells/mL) was pipetted onto the top of each ring and incubated for 1 h. This procedure was repeated once after rotating the sylgard tube 180°. An additional 48 h of static incubation preceded final positioning of the entire assembly into the bioreactor system. The bioreactor system consisted of a gear pump (Ismatec, Glattbrugg, Switzerland) controlled by a program written in Labview (NI instruments, Austin, TX). The gear pump supplied a pulsatile flow waveform at a frequency of 1.0 Hz that induced a 5% strain in the sylgard tube. Flow through the conduit is monitored and recorded by a flow meter (TS 410; Transonic, Ithaca, NY) and a pressure transducer (Millar Instruments, Houston, TX). This bioreactor system was set up in an incubator maintained at 37°C and 5% CO_2. Upon the completion of the bioreactor preconditioning (7 and 14 days), individual rings were removed, and H&E and DAPI staining were performed to determine the proliferation and migration of the VSMCs.

Fura-2–based digital imaging microscopy

Preconditioned seeded decellularized ring segments were removed from the bioreactor and incubated in serum-free media for 48 h before calcium imaging. Segments were loaded with the calcium-specific fluorescent dye fura-2 AM (5 μM mixed with equal volume of 10% w/v Pluronic F-127) by incubating at room temperature in serum-free medium for 1 h. Segments were then washed with Krebs buffer and pinned over small rectangular blocks made of sylgard. These blocks were then laid over cover slip–bottomed dishes with the cellular portion of the recellularized segment facing down toward the objective of inverted microscope (Zeiss, Oberkochem, Germany).

Fura-2 images were obtained using a computer-controlled monochromatic excitation light source (Polychrome II; TILL Photonics, Martinsried, Germany) and a cooled charge-coupled device camera with exposure control (SensiCam; Till Photonics). During excitation at 340 or 380 nm, emission at 510 nm was collected by the camera for 300 ms. A 340/380 ratio image was generated after background subtraction using Till Vision software (TILL Photonics). Fura-2 ratio image intensity was expressed as relative fluorescence units evaluated by Till Vision software. Ratio images were obtained before treatment and at regular intervals of 15 s after treatment with 60 mM KCl.

Histology and immunostaining

Recellularized graft segments were embedded and frozen in optimal cutting temperature (O.C.T.) compound medium (Tissue-Tek, Torrance, CA) and cut cross-sectionally into 8 μm sections. H&E (Sigma-Aldrich, St. Louis, MO) and nuclear DAPI (Vector, Burlingame, CA) staining were used for histological evaluation of the seeded decellularized grafts. For the Movat staining, a modified Movat Pentachrome method was used.[14]

SMCs were identified by microscopy using antibodies specific for VSMCs. Passage 1 SMCs were fixed for 10 min in 4% paraformaldehyde (Sigma, St. Louis, MO) on a six-well culture dish. Cells were then permeabilized with 2% Triton ×100 (Sigma) for 5 min. Nonspecific binding sites were saturated by 15 min of incubation with 2% fetal calf serum. Cells were then incubated overnight at 4°C with primary antibodies to α-smooth muscle actin (1:50; Santa Cruz, Santa Cruz, CA) and SMC myosin heavy chain (1:50; Santa Cruz) in 2% fetal calf serum. After repeated wash in phosphate-buffered saline, cells were then incubated for 1 h at room temperature with a species-specific secondary antibody (1:100; Jackson ImmunoResearch Lab, West Grove, PA). The nuclei were counter stained with hematoxylin, and microscopy was performed using a Carl Zeiss microscope.

Morphometry and statistical analysis

Morphometric software (IPLab for Mac OS X; BD Biosciences–Bioimagaing, Rockville, MD) was calibrated using National Institute of Standards and Technology (NIST) traceable microscope stage micrometers of 2.0 mm linear and 2.0 mm diameter circle with all objectives. Klarmann Rulings, Inc. (Manchester, NH) certified all micrometer graduations. Quantification of the SMC layer thickness was measured with digital morphometry as follows: the SMC layer thickness was measured using IPLab software (line tool) where a digital image of the histological section (H&E) is used. The length of the cell layer is measured in pixels and converted to microns. The number of SMCs was quantified in a similar fashion using DAPI staining. That is, the SMC cell count was also performed using IPLab software (segment tool) where individual cells on DAPI-stained sections were counted. In addition, the

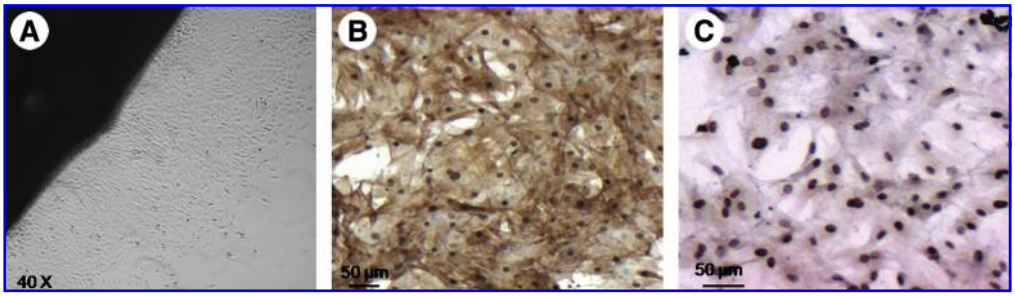

FIG. 1. Homogeneity of cultured SMCs derived from explanted rat aorta. (**A**) Phase contrast images demonstrating primary cultured cells growing from explanted segments of rat aorta (40×). (**B**) Micrograph images of primary cultured cells stained with anti-α-SMA (100×). (**C**) Micrograph images of primary cultured cells stained with anti-SMC myosin heavy chain (100×). Color images available online at www.liebertonline.com/ten.

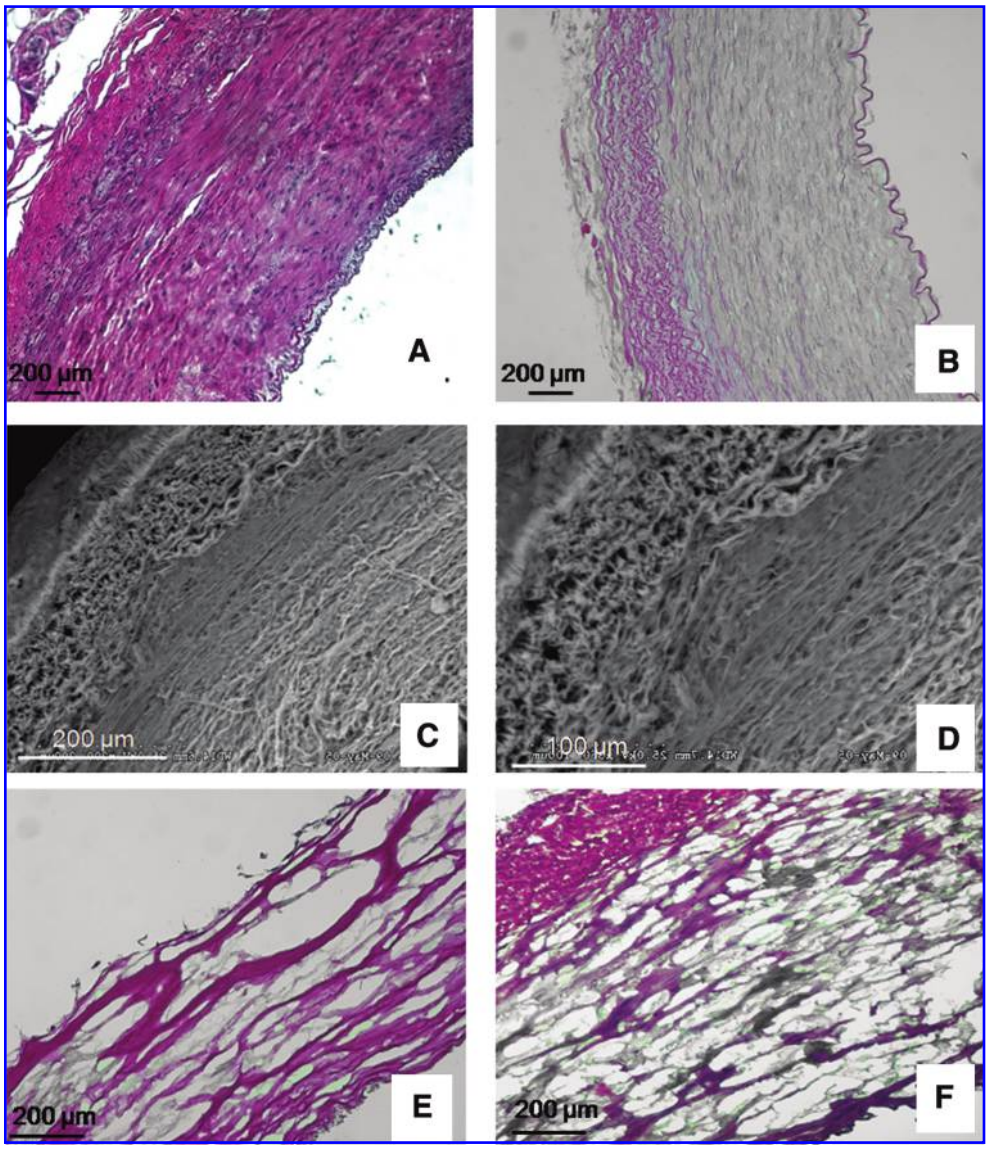

FIG. 2. Decellularization of porcine carotid arterial segments. (**A**) H&E image of native porcine carotid artery (40×). (**B**) H&E image of a decellularized porcine carotid artery (40×). (**C, D**) Representative SEM images of decellularized porcine carotid artery (magnification was 200× and 350×, respectively). (**E**) H&E image adventitia-denuded, decellularized porcine carotid artery (100×). (**F**) H&E image of a decellularized porcine carotid artery (100×). Color images available online at www .liebertonline.com/ten.

length of the surface was also measured to determine the cell density (no. of counts/mm^2). For these measurements, the thickness of the segment was assumed to be 5 μm. In both cases, the continuous data were expressed as mean mean ± SD. Statistical comparison of the parameters was performed using a Student's *t*-test for unpaired samples. A *p*-value ≤0.05 was considered statistically significant.

Biomechanical testing

Mechanical loading test on the scaffolds was performed using a uniaxial load frame (Instron, Issaquah, WA) in circumferential direction. A 1-cm-long ring was cut from the scaffold or native artery and opened into a strip and clamped at each end. The crosshead speed was set as 0.5 mm/s. Young's modulus was calculated from the slope of linear region of stress–strain curve. Data were analyzed by a one-way ANOVA with a Tukey *post hoc* test used for pairwise comparisons.

Results

SMC cultures

Figure 1 shows the homogeneous VSMC cultures obtained from explanted rat aortic ring segments. As illustrated, cells migrated from the tissue, attached, and grew to confluence on cell culture plates within 7 days. At confluence, cells were trypsinized, resuspended in fresh media, and cultured in 10 cm tissue cultured dishes for further passaging. During this time, VSMCs stained for both smooth muscle actin and smooth muscle myosin heavy chain (Fig. 1).

Decellularization process and adventitial removal

To obtain more porous rings, we decellularized segments of porcine common carotid arteries (Fig. 2). These segments possessed an internal luminal diameter of ≈3–4 mm and were ≈5 mm in length. Arterial segments subjected to decellularization and lyophilization maintained their tubular appearance and did not shrink significantly. H&E staining of decellularized vessels showed multiple layers of collagenous fibers within the vessel walls (Fig. 2B). These results demonstrate that the decellularization process removed all the native cells from the vessel, leaving a porous collagenous matrix. SEM images depict the obvious distinctions between the adventitial and medial smooth muscle layers (Fig. 2C, D). Thus, to provide improved access to the media layer during VSMC seeding, the adventitia was removed from the decellularized porcine carotid arteries (see Materials and Methods; compare Fig. 2E, F).

Biomechanical properties

Stress–strain curves were developed from tensile testing for scaffolds with adventitia ($n=7$) and without adventitia ($n=5$), as well as from native porcine carotid arteries ($n=7$). As illustrated, removal of the adventitial layer had a modest impact on the biomechanical properties of the decellularized

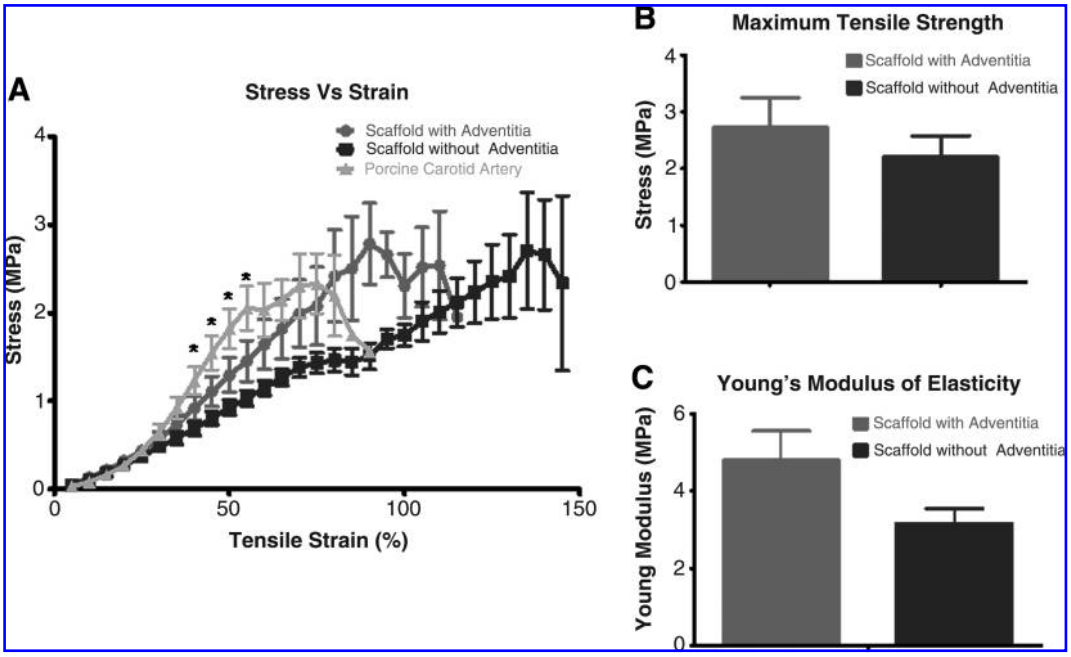

FIG. 3. Comparison of biomechanical characteristics of native porcine carotid artery ($n=7$) and decellularized porcine carotid artery in the absence ($n=5$) and presence ($n=7$) of adventitia. Panel (**A**) shows the stress–strain relationship for all three preparations, where asterisks (*) indicate a statistically significant difference between the native artery and the adventitia-free scaffold, $p<0.05$, one-way ANOVA with a Tukey *post hoc* pairwise comparisons. Note: there were no significant differences detected between adventitia-intact scaffolds and native arteries or adventitia-free scaffolds. Panels (**B**) and (**C**) plot the average maximal tensile strength and Young's modulus, respectively, observed in decellularized vessels in that absence and presence of adventitia. Again, statistical analysis did not reveal any significant differences in these measures ($p>0.05$ in all cases). These observations clearly document the relative biomechanical equivalence of these preparations (see Results and Discussion sections for more details).

scaffold (Fig. 3A). More specifically, while some statistical differences were found between native artery and adventitia-free scaffolds, there were no differences between the adventitia-intact and adventitia-denuded scaffolds, and the statistically significant differences that were detected occurred over a narrow range of values (between 40% and 55% strain) outside the range considered to be physiologically relevant (i.e., 10–20%).[15] Consistent with these observations, there was no significant difference in either the maximal tensile strength or Young's modulus between the adventitia-intact and -denuded decellularized scaffolds (Fig. 3B, C).

Static seeding

Static seeding experiments were performed on more than 100 scaffolds and were assessed at time points ranging in duration from 1 h to 7 days. Figure 4 shows representative examples of results obtained in the presence (Fig. 4A, B) and absence (Fig. 4C, D) of adventitia 24 h and 1 week (Fig. 4E, F), respectively, after VSMC seeding. There are two important points to note here: (i) as shown in Figure 4E and F, there was little difference if the seeded scaffolds were left under static conditions for up to 1 week; (ii) overall, the data clearly demonstrated that VSMCs adhered to the media layer more readily than to the adventitia layer.

VSMC seeding and bioreactor preconditioning

Approximately 3 mm rings of decellularized scaffolds were placed on a custom-made elastomeric silicone tube and seeded with VSMCs (Fig. 5). Forty-eight hours after seeding, the constructs were placed in a bioreactor system (Fig. 5), and subjected to mechanical strain. The conditions consisted of a pulse rate of 60 beats/min and a pressure range of 80–120 mmHg. Seeded scaffolds were maintained in this preconditioning protocol for a duration of either 7 or 14 days. A subset of recellularized scaffolds was maintained under static conditions for an equivalent period of time to serve as time-matched controls. H&E staining of scaffold cross sections clearly documented the benefits of 1 week of mechanical stimulation on cellular proliferation in either the presence or absence of the adventitial layer. Representative examples are shown in Figure 6 (compare Fig. 6A, B, with 6C, D, respectively). The results of DAPI staining also demonstrated the enhanced cellularization obtained in the absence of the adventitia (see Fig. 6E, F). Finally, H&E and

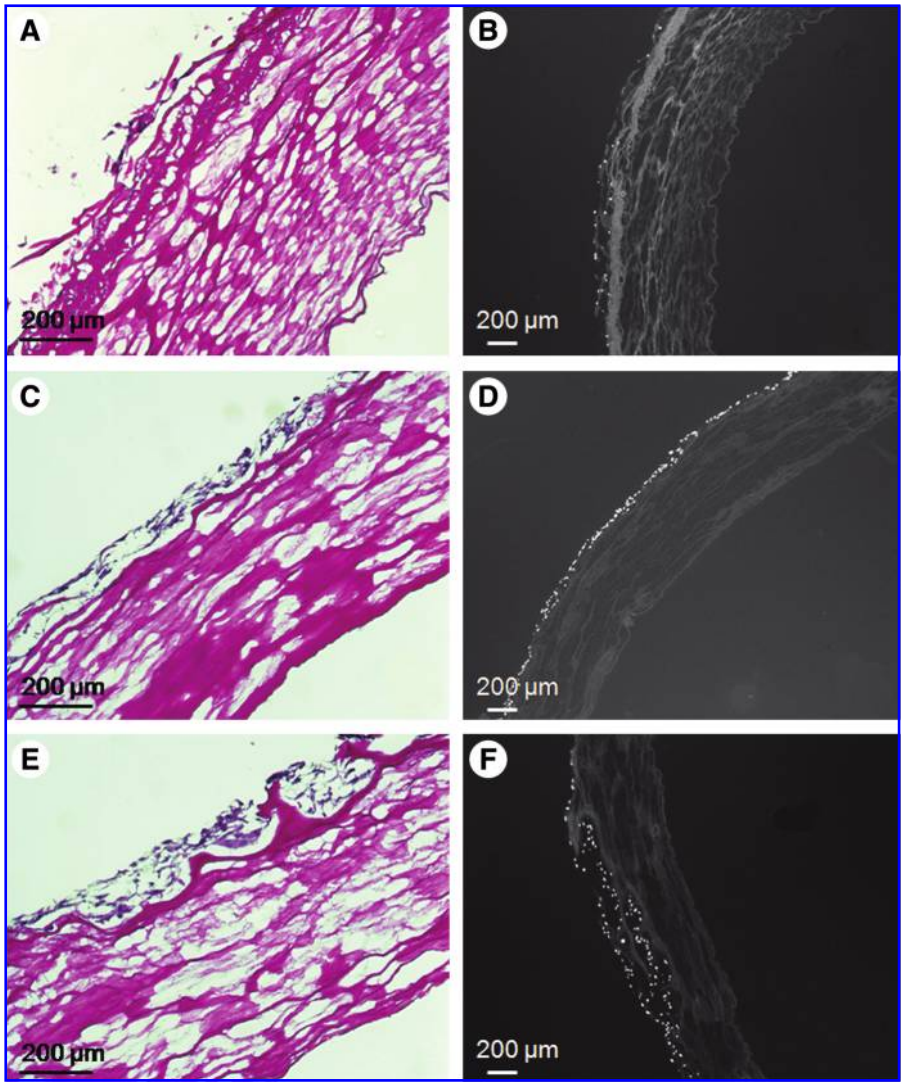

FIG. 4. Representative photomicrographs demonstrating the impact of removing the adventitia layer on VSMC seeding. (**A**) H&E image taken 24 h after VSMCs seeding onto an adventitia-intact scaffold (100×). (**B**) DAPI image taken 24 h after VSMCs seeding onto an adventitia-intact scaffold (50×). (**C**) H&E image taken 24 h after VSMCs seeding onto an adventitia-denuded scaffold (100×). (**D**) DAPI image taken 24 h after VSMCs seeding onto an adventitia-denuded scaffold (50×). (**E**) H&E image taken 1 week after VSMCs seeding onto an adventitia-denuded scaffold (100×). (**F**) DAPI image taken 1 week after VSMCs seeding onto an adventitia-denuded scaffold (50×). Color images available online at www.liebertonline.com/ten.

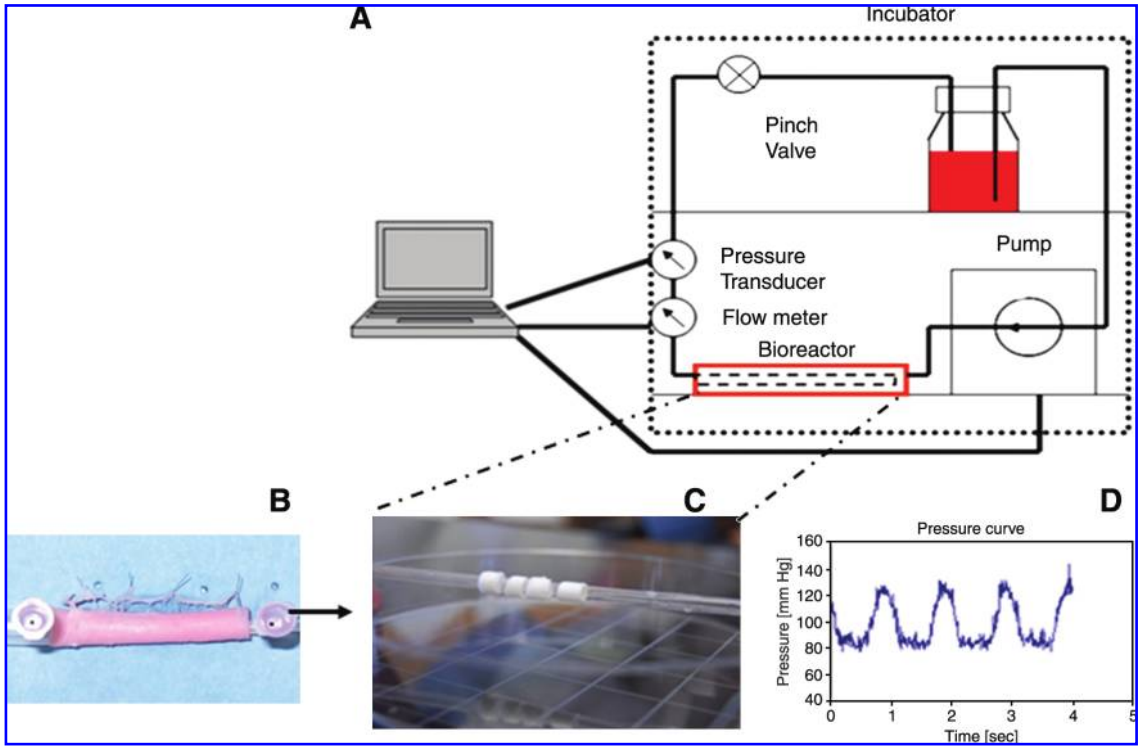

FIG. 5. Schematic depiction of the bioreactor system used for preconditioning of VSMC-seeded rings of engineered vessel. (**A**) Illustration of the flow system setup to induce cyclic strain onto the engineered vessels. (**B**) Removal of adventitial layer. (**C**) Snap image demonstrating the position of the vascular rings on the custom sylgard tube. (**D**) Corresponding pressure measurements of the bioreactor system. Color images available online at www.liebertonline.com/ten.

DAPI staining (compare Fig. 6G, H with 6I, J, respectively) documented that increasing the bioreactor preconditioning protocol from 1 to 2 weeks provided further improvements in cellular proliferation and tissue formation, again, in either the presence or absence of adventitia. Consistent with these visual observations, statistical analysis of cell density data also revealed a significant impact of adventitia removal on cellular proliferation (see Materials and Methods). Mean quantitative data for several such experiments are plotted in Figure 7. However, at 2 weeks, the cellular densities on the adventitia-intact and -denuded scaffolds were equivalent. Figure 8 provides other representative examples of the enhanced VSMC layer achieved after 2 weeks of bioreactor preconditioning, as well as an example of the impact of 3 weeks of bioreactor preconditioning. Moreover, morphometric analysis of the thickness of the VSMC layer once again revealed a significant increase in VSMC wall thickness at 1 week, but relatively equivalent VSMC layers after 2 weeks of bioreactor preconditioning (Fig. 9). Taken together, the results clearly demonstrate that the bioreactor preconditioned VSMCs responded to the cyclic strain by proliferating and organizing into a medial SMC layer by day 14 (Figs. 6–9). Moreover, removal of the adventitial layer resulted in an accelerated cellular proliferation and enhanced VSMC wall thickness at the 1-week time point. In addition, as shown in Figure 10, during bioreactor preconditioning, the developing VSMC layer is capable of remodeling the scaffold and depositing extracellular matrix, as reflected by the presence of significant elastin and proteoglycan staining, respectively.

Fura-2–based digital imaging microscopy of steady-state intracellular calcium levels

After 1 and 2 weeks of bioreactor preconditioning, cells were loaded with the membrane permeant calcium-sensitive dye Fura-2 (see Materials and Methods). Interestingly, there was no detectable response in any scaffold at any time point to the addition of phenylephrine, serotonin, or endothelin-1. However, as illustrated in Figure 11, after 1 week of bioreactor preconditioning, VSMCs from both adventitia-intact and -denuded scaffolds displayed depolarization-induced increases in steady-state intracellular calcium levels. However, after 2 weeks of bioreactor preconditioning, only VSMCs on the adventitia-denuded scaffolds retained their ability to mobilize calcium in response to KCl-induced depolarization. Similar results were observed in two other independent experiments at the 2-week time point.

Discussion

The initial clinical use of vascular constructs engineered *in vitro* and subsequently implanted *in vivo* without a functional medial SMC layer has been reported.[16] Nonetheless, the long-term success of this approach has not been determined; therefore, the continued development of a tissue-engineered blood vessel that more closely mimics the current gold standard for vascular replacement, that is, native autologous vessel, remains an important medical research objective. In this regard, the pursuit of engineered vessels that possess native vascular composition, mechanics, and physiology/function clearly poses a great technical challenge[10,17–20]

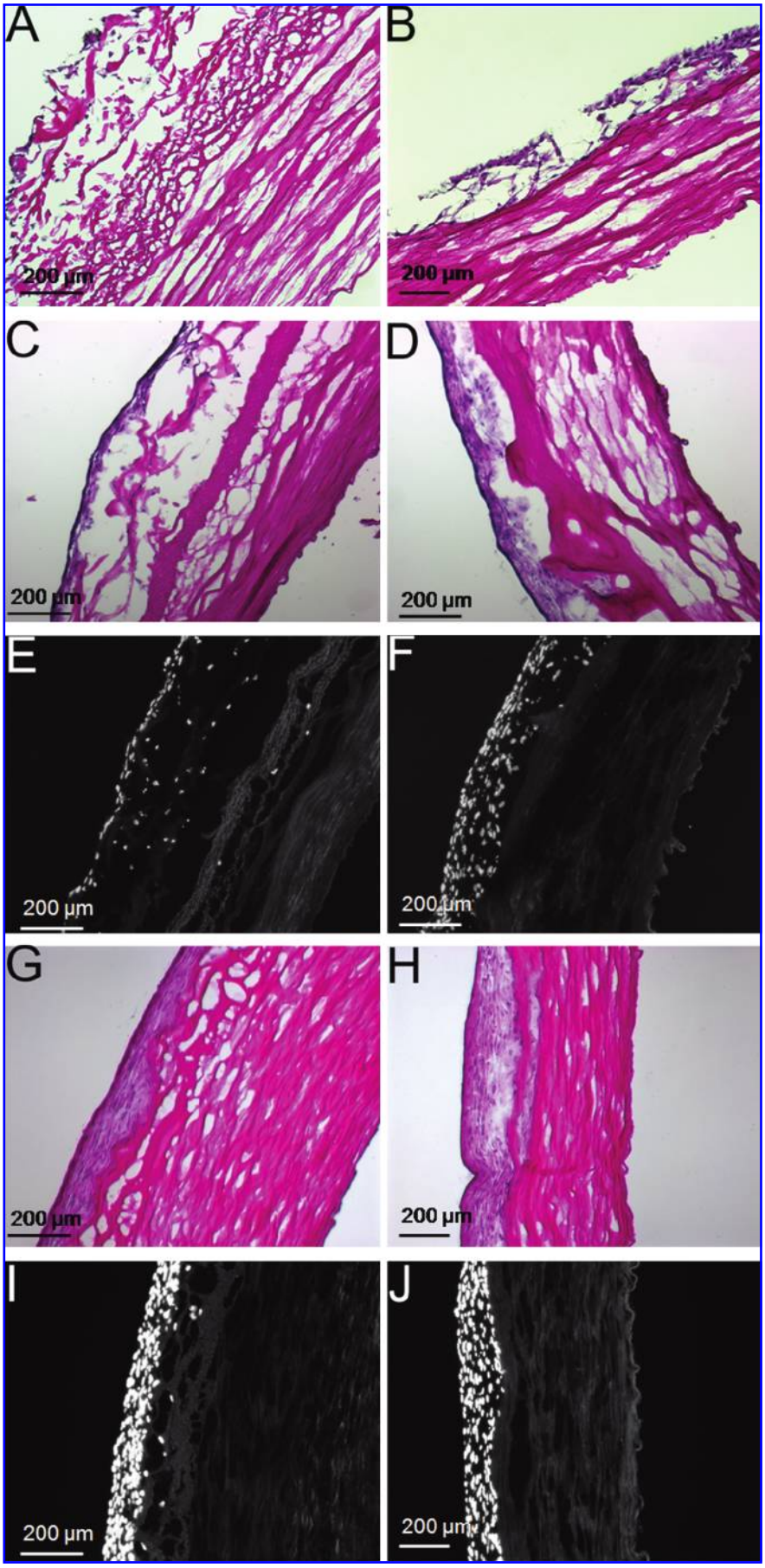

FIG. 6. Representative examples of the impact of adventitia removal and bioreactor preconditioning on development of a medial smooth muscle layer. All panels on the left (**A, C, E, G, I**) depict results obtained on adventitia-intact scaffolds, while all panels on the right (**B, D, F, H, J**) depict results obtained on adventitia-denuded scaffolds. (**A, B**) H&E images of VSMCs 7 days after static seeding (i.e., no bioreactor preconditioning). (**C, D**) H&E images of statically seeded VSMCs after 7 days in the bioreactor. (**E, F**) DAPI images of statically seeded VSMCs after 7 days in the bioreactor. (**G, H**) H&E image of statically seeded VSMCs after 14 days in the bioreactor. (**I, J**) DAPI images of statically seeded VSMCs after 14 days in the bioreactor. 100× magnification in panels (**A–J**). Color images available online at www.liebertonline.com/ten.

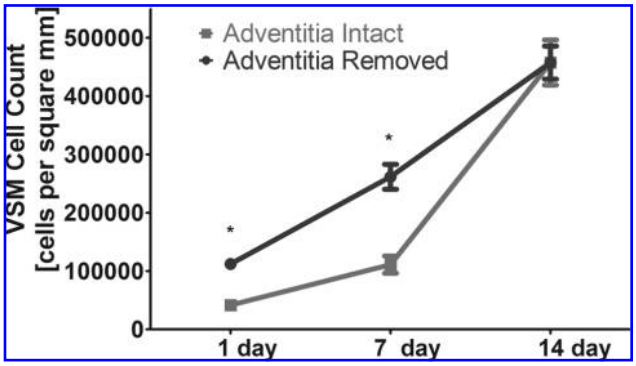

FIG. 7. Graphical plot of the impact of bioreactor preconditioning and adventitial removal on cell proliferation on the decellularized scaffold. Significant differences were observed between adventitia-intact and -denuded preparations at both the 1- and 7-day time points, where asterisks (*) indicate a statistically significant different, $p < 0.05$, Student's *t*-test for unpaired samples. $n = 3$ sections evaluated for all plotted points (see Materials and Methods for details).

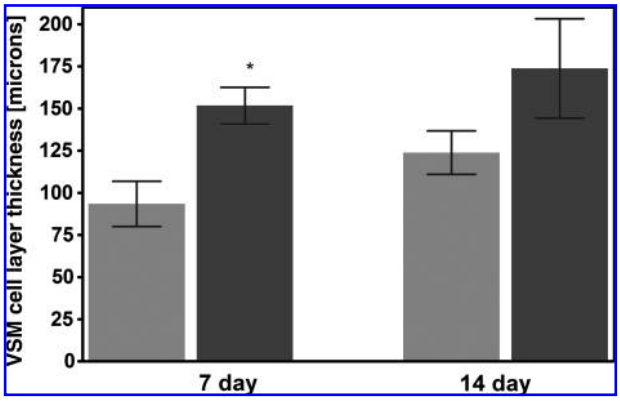

FIG. 9. Graphical plot of the impact of bioreactor preconditioning and adventitial removal on the thickness of the medial VSMC layer. Significant differences were observed between adventitia-intact and -denuded preparations at the 7-day time point, where asterisk (*) indicates a statistically significant different, $p < 0.05$, Student's *t*-test for unpaired samples. $n = 3$ sections evaluated for all plotted points (see Materials and Methods for details).

although the importance and benefits of so doing have been codified.[21–23] In this scenario, *in vitro* vessel engineering may represent a critical step in the optimization of vascular grafts for subsequent implantation *in vivo*. Again, the major scientific roadblock that remains is the inability to generate a physiologically relevant medial SMC layer, though progress has been made in this regard.[9,10,22] This barrier, in turn, reflects the absence of reliable *in vitro* methods for seeding sufficient numbers of VSMCs onto and into scaffolds (either synthetic or natural) to ensure formation of a multilayer media, while simultaneously ensuring that sufficient numbers of VSMCs assume and retain a contractile phenotype rather than a proliferative phenotype.[24] Not surprisingly, few groups have been successful in developing functional vascular tissue, even with improved bioreactor design, long preconditioning protocols, and prolonged culture times.[9,12,13,17,18,22,25] We report here some initial steps in this direction, by defining a methodology for obtaining muscularized (i.e., multilayer VSMCs) tissue-engineered blood vessels derived from explanted rat aortic VSMCs seeded on decellularized porcine carotid arteries.

The importance of the medial layer of the vessel wall

In this regard, a few important novelties have resulted from these initial investigations. First, we report that the magnitude of the impact of bioreactor preconditioning on SMC proliferation is accelerated by surface modification (i.e., removal of the adventitia) of the scaffold (Figs. 6–10). More specifically, we observed a two- to threefold increase in cell number/wall thickness at initial seeding (i.e., 1 day) as well as after 7 days of bioreactor preconditioning. Such observations may have major implications to the time required for vessel engineering, and thus, to the eventual cost of vascular replacement. In fact, we are not aware of any publication that reports an SMC layer in an engineered tabularized tissue, that is, 150–200 μm thick *in vitro* as reported herein, the equivalent of ≈15 cell layers after 2 weeks of bioreactor preconditioning. We believe that this is an important and novel achievement. Second, the calcium imaging data clearly emphasize that even when one has a substantial medial SMC layer, this does not imply that the signal transduction

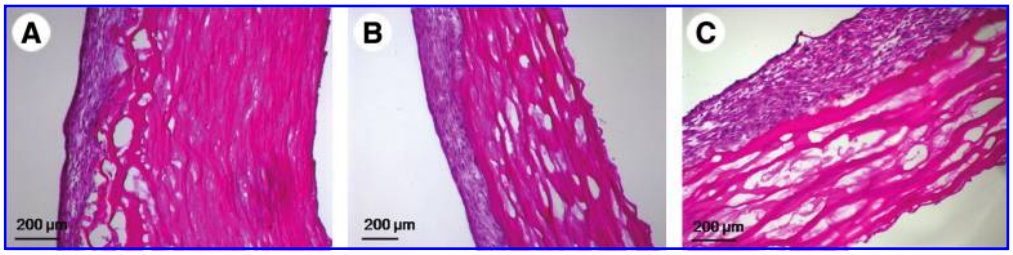

FIG. 8. Representative examples of H&E images demonstrating the capacity of bioreactor preconditioning to produce a multilayer medial smooth muscle layer. (**A**) H&E image depicting the impact of 2 weeks of bioreactor preconditioning on VSMC proliferation and maturation on an adventitia-intact scaffold (100×). (**B**) H&E image depicting the impact of 2 weeks of bioreactor preconditioning on VSMC proliferation and maturation on an adventitia-denuded scaffold (100×). (**C**) H&E image depicting the impact of 3 weeks of bioreactor preconditioning on VSMC proliferation and maturation on an adventitia-denuded scaffold (100×). Color images available online at www.liebertonline.com/ten.

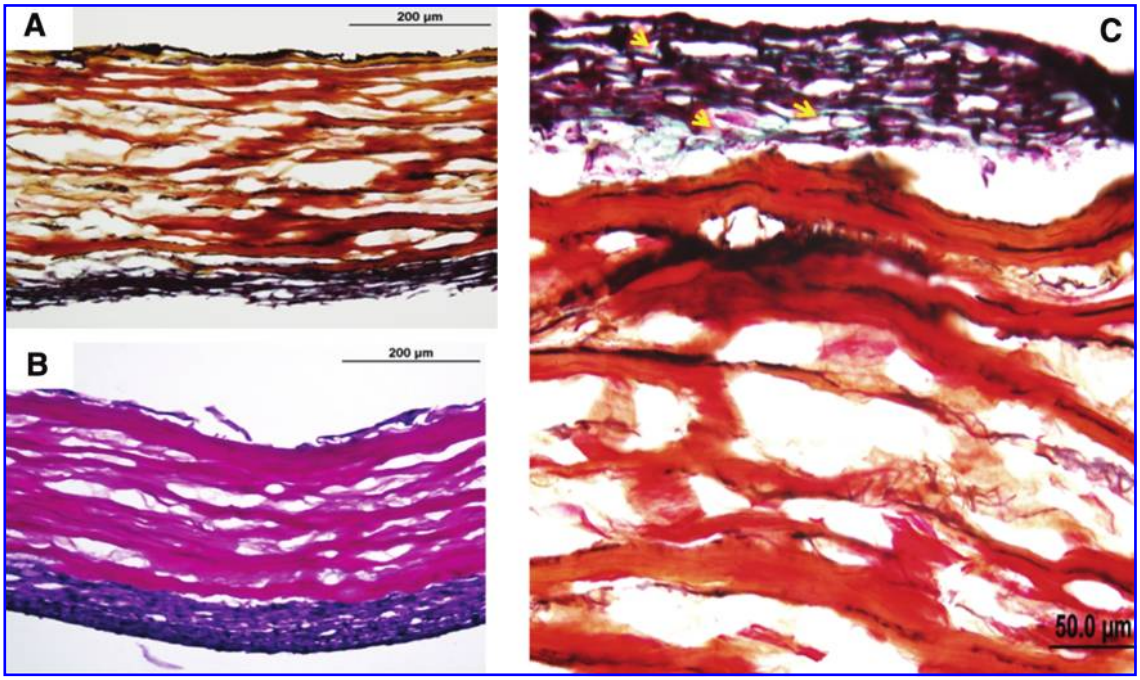

FIG. 10. Representative examples of the impact of bioreactor preconditioning on remodeling/extracellular matrix deposition among/near the VSMC layer in adventitia-denuded preparations. Panels (**A**) and (**B**) depict H&E and Movat staining of 1 week bioreactor preconditioned scaffolds without adventitia (magnification 200×). Panel (**C**) shows a higher magnification image of Movat staining revealing the presence of proteoglycan content (arrows) deposited within the preconditioned SMC layer (proteoglycan content is shown in green at magnification 400×). Color images available online at www.liebertonline.com/ten.

mechanisms responsible for contraction are present and physiologically relevant at the cellular level. Presumably, this observation explains why no more than 5% of native vessel contraction has been observed *in vitro* in a bioengineered vessel to date. Third, it is important to keep in mind that even in the presence of an equivalent cell number/wall thickness (i.e., at the 2-week time point in the adventitia-denuded and adventitia-intact scaffolds), the muscle cell/wall thickness ratio is still more favorable in the absence than the presence of adventitia. This latter observation is of

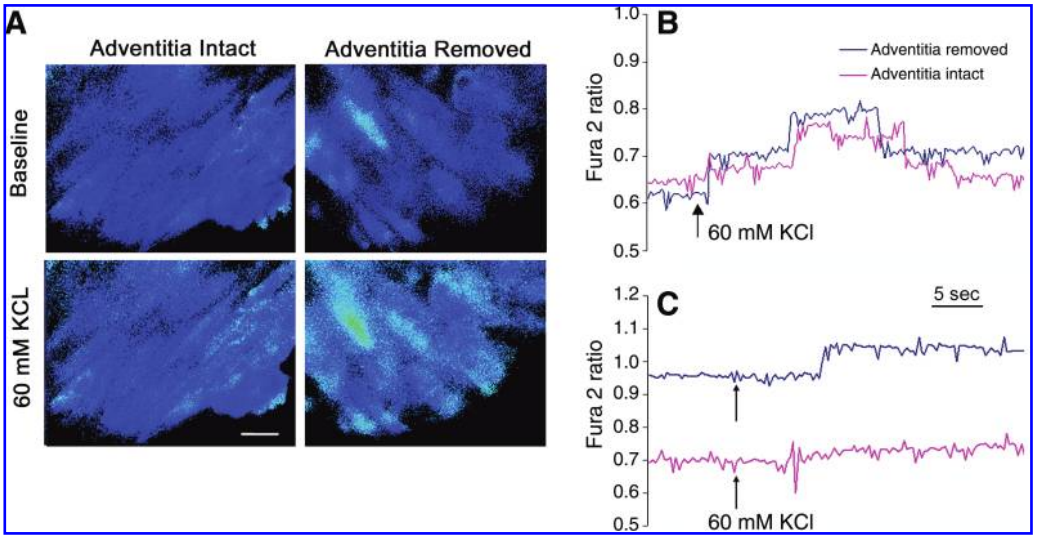

FIG. 11. Digital imaging microscopy of intracellular calcium mobilization in Fura-2–loaded engineered vessels after bioreactor preconditioning. (**A**) Representative Fura-2 psuedocolored ratio images obtained at baseline and after addition of 60 mM KCl after 2 weeks of bioreactor preconditioning. Also shown are the time course of the alterations in the steady-state Fura-2 ratio in response to addition of 60 mM KCl in two other experiments, one each in adventitia-intact and -denuded engineered vessels after 1 (**B**) and 2 weeks (**C**) of bioreactor preconditioning. Color images available online at www.liebertonline.com/ten.

physiological significance both to the ability of SMC contraction to be functional, as well as for the smaller degree of remodeling required to obtain more native vessel architecture (either *in vitro* or *in vivo*). It is also worth noting that reendotheliliazed decellularized scaffolds have lasted up to 130 days after implantation as a carotid artery interposition graft *in vivo*.[26] In light of the apparent biomechanical equivalence of the decellularized vessel wall in the absence and presence of the adventitia *in vitro* (Fig. 3), particularly in the physiologically relevant range of strain (10–20%[15]), such surface modification appears quite beneficial to the vessel tissue engineering process.

Some of these observations regarding the apparent impact of the adventitia on the acceleration of the tissue engineering process may be explained by the fact that the adventitia of muscular arteries has a significantly different composition than the medial layer. For example, collagen is the major extracellular component of the adventitia, whereas the media layer contains more elastin and laminin. These three proteins influence the fate of SMCs differently. More specifically, collagen has been shown to shift VSMCs phenotype toward the synthetic phenotype.[27] In contrast, SMCs seeded on laminin and elastin better maintain functional characteristics of VSMCs.[28,29] Consistent with this supposition, Figure 10 illustrates that in the absence of the adventitia, VSMCs appear capable of remodeling the existing scaffold. For example, the deposition of detectable elastin (Fig. 10A, black staining) and proteoglycan (Fig. 10C, green staining) can be seen in the VSMC layer after bioreactor preconditioning. In summary, the representative Movat staining reported in these initial studies clearly identifies the internal elastic lamina and external elastic lamina, as well as new extracellular matrix material (i.e., proteoglycans). Similar observations were made on the adventitia-intact preparations (data not shown). In any event, when taken together with the biomechanical data (Fig. 3), these data indicate that the engineered vessels reported herein possess the critical structural components required for maintaining strength, durability, and the like.

The importance of cyclic bioreactor preconditioning to development of a multilayer smooth muscle morphology

The benefits of incorporation of mechanical cyclic strain to the distribution and enhanced phenotypic characteristics of VSMCs in engineered blood vessels have been documented.[9,20,21,30–35] In fact, there is also a large body of data that has employed one of several types of mechanical stretch devices to simulate the mechanical strains present in blood vessels at different locations in the vascular tree and thus evaluate the impact of cyclic strain on a variety of phenotypic characteristics of SMC differentiation.[36–41] However, the primary evaluation endpoint of virtually all of these studies has been at the molecular, immunochemical, or histological levels. That is, most investigations have evaluated the impact of cyclic strain on markers/indices of VSMC growth and differentiation, rather than focusing on the function, that is, the contractility of the VSMCs, with rare exception.[9,22]

In this regard, the current report demonstrates that mechanical strain was induced by an increase in pressure, which in turn expanded the silicone tube and stretched the seeded scaffold radially (Fig. 5). This provides a system where the seeded cells only experience mechanical strain, not shear stress and/or chemotaxis. Moreover, the current bioreactor design also provides an opportunity to study multiple samples under the same experimental conditions, providing important longitudinal (i.e., time dependent) information.

Again, while it is documented that cyclic mechanical parameters such as strain magnitude, frequency, and time of exposure (i.e., duration) affect the behavior of seeded VSMCs,[24,31,33,42,43] in our studies, normal physiological frequency (60 beats/min) and pressure (80–120 mmHg) parameters were used to determine the effects of cyclic strain on the optimized seeded grafts. From our current results, we can also conclude that cyclic preconditioning is a very effective method for inducing cellular proliferation and alignment of a multilayer VSMC media (150–200 μM thick; Figs. 6–9). So, what mechanism(s) might account, at least in part, for this observation? An increase in glycosaminoglycan and proteoglycan synthesis[44–46] in VSMCs, for example, has been shown with application of cyclic strain. Glycosaminoglycan and proteoglycan, in turn, have both been shown to affect VSMCs growth.[47] Moreover, the expression and secretion of growth factors and signaling molecules from VSMCs, that is, transforming growth factor beta, platelet-derived growth factor, and vascular endothelial–derived growth factor,[48–50] has also been shown to be increased due to mechanical strain. All of these molecules have also been shown to regulate VSMCs growth and collagen synthesis,[51] and such effects may account, at least in part, for the current observations. As noted above and consistent with these prior reports, our current data document that bioreactor preconditioning is associated with the presence of newly synthesized extracellular matrix material.

Intracellular calcium mobilization in VSMCs after bioreactor preconditioning

Another important aspect of the current investigation is that we endeavored to begin to study the impact of bioreactor preconditioning on signal transduction in VSMCs. The scientific rationale for this approach is related to the fact that the observation of pharmacological responses presumes the presence of receptors for circulating hormones as well as those for agents secreted by native neuronal innervation, as would be required for normal vascular function *in vivo*. In fact, there is little information available concerning the impact of cyclic bioreactor preconditioning on the pharmacological fingerprint of bioengineered vessels, and as indicated herein, it is conceivable that the tissue may be pharmacologically numb. Because of the well-established link between increases in intracellular calcium levels and increased contraction of VSMCs, we examined the response of Fura-2–loaded preparations to both receptor- and nonreceptor-mediated cellular activation. In this regard, there was no evidence for the presence of receptor-mediated intracellular calcium signaling in the muscularized arteries, at least as revealed by commonly used and physiologically relevant vasoactive agents. Specifically, there were no detectable intracellular calcium responses to phenylephrine (α_1-adrenergic receptor agonist, 10 μM), serotonin (5-HT_2 receptor agonist, 10 μM), or endothelin-1 (ET-1_A receptor agonist, 100 nM) (data not shown). However, intracellular calcium mobilization in VSMCs was detected in response to depolarization with

60 mM KCl (see Fig. 11). While we are cautious not to overinterpret these initial observations, these data are consistent with the hypothesis advanced above; that is, the receptor-mediated activation pathways are either absent or uncoupled to intracellular calcium signaling in these muscularized constructs; that is, the engineered vessels are pharmacologically numb. Nonetheless, there is still clear evidence for the presence of the L-type voltage-dependent calcium channel.

In addition, more robust and reproducible KCl-mediated intracellular calcium responses were observed in muscularized constructs without adventitia than in muscularized constructs in the presence of adventitia (Fig. 11). While further experiments are clearly required to better understand the nature of this phenomenon, it seems reasonable to posit that the scaffold and preconditioning protocol have a significant, albeit penultimate with respect to native vessel function, impact on cellular physiology. To summarize then, these observations confirm and extend prior studies where, in general, three-dimensional matrices, as compared to two-dimensional environments, have been shown to prolong functional behavior of the VSMCs[34,52,53]; moreover, the presence of extracellular matrix proteins such as elastin, laminin, and collagen have also been shown to be beneficial to cell seeding and function.[28,29,54]

In conclusion, we have identified bioreactor conditions, seeding methods, and structural modifications (i.e., adventitia removal) sufficient to ensure more optimized static seeding of engineered constructs by VSMCs, resulting in the presence of a thick, multilayered media. The apparent benefits of cyclic bioreactor preconditioning, in combination with removal of the adventitial layer to the accelerated formation of a muscularized engineered vessel, appear quite promising. However, this important initial observation requires further investigation to determine any specific scaffold surface proteins and bioreactor conditions that might be responsible for mediating the observed effects. Moreover, one major goal of future experiments is to further refine the experimental conditions (i.e., adjustment and fine-tuning of bioreactor protocols, media supplements, scaffold preparation, etc.) to further enhance the functional characteristics of the bioengineered vessel, in particular with respect to more enhanced investment of VSMCs throughout the wall of the scaffold. The long-term goal is to develop engineered blood vessels for vascular replacement that more closely mimic native vasculature both *in vitro*, as well as when implanted—that is, vessels that possess a functional receptor-mediated signal transduction apparatus and a capacity for physiologically relevant contraction.

Acknowledgment

This work was supported in part by a grant from Tengion, Inc.

Disclosure Statement

No competing financial interests exist.

References

1. Weinberg, C.B., and Bell, E. A blood vessel model constructed from collagen and cultured vascular cells. Science **231,** 397, 1986.
2. Teebken, O.E., and Haverich, A. Tissue engineering of small diameter vascular grafts. Eur J Vasc Endovasc Surg **23,** 475, 2002.
3. Ratcliffe, A. Tissue engineering of vascular grafts. Matrix Biol **19,** 353, 2000.
4. Dora, K.A. Cell-cell communication in the vessel wall. Vasc Med **6,** 43, 2001.
5. Yu, H., Wang, Y., Eton, D., Rowe, V.L., Terramani, T.T., Cramer, D.V., Starnes, V.A., and Weaver, F.A. Dual cell seeding and the use of zymogen tissue plasminogen activator to improve cell retention on polytetrafluoroethylene grafts. J Vasc Surg **34,** 337, 2001.
6. Di Luozzo, G., Bhargava, J., and Powell, R.J. Vascular smooth muscle cell effect on endothelial cell endothelin-1 production. J Vasc Surg **31,** 781, 2000.
7. Opitz, F., Schenke-Layland, K., Richter, W., Martin, D.P., Degenkolbe, I., Wahlers, T., and Stock, U.A. Tissue engineering of ovine aortic blood vessel substitutes using applied shear stress and enzymatically derived vascular smooth muscle cells. Ann Biomed Eng **32,** 212, 2004.
8. Li, C., Hill, A., and Imran, M. *In vitro* and *in vivo* studies of ePTFE vascular grafts treated with P15 peptide. J Biomater Sci Polym Ed **16,** 875, 2005.
9. Niklason, L.E., Gao, J., Abbott, W.M., Hirschi, K.K., Houser, S., Marini, R., and Langer, R. Functional arteries grown *in vitro*. Science **284,** 489, 1999.
10. Gong, Z., and Niklason, L.E. Blood vessels engineered from human cells. Trends Cardiovasc Med **16,** 153, 2006.
11. Badylak, S.F., Lantz, G.C., Coffey, A., and Geddes, L.A. Small intestinal submucosa as a large diameter vascular graft in the dog. J Surg Res **47,** 74, 1989.
12. McFetridge, P.S., Bodamyali, T., Horrocks, M., and Chaudhuri, J.B. Endothelial and smooth muscle cell seeding onto processed *ex vivo* arterial scaffolds using 3D vascular bioreactors. ASAIO J **50,** 591, 2004.
13. Zhu, C., Ying, D., Mi, J., Li, L., Zeng, W., Hou, C., Sun, J., Yuan, W., Wen, C., and Zhang, W. Development of anti-atherosclerotic tissue-engineered blood vessel by A20-regulated endothelial progenitor cells seeding decellularized vascular matrix. Biomaterials **29,** 2628, 2008.
14. Finn, A.V., Joner, M., Nakazawa, G., Kolodgie, F., Newell, J., John, M.C., Gold, H.K., and Virmani, R. Pathological correlates of late drug-eluting stent thrombosis: strut coverage as a marker of endothelialization. Circulation **115,** 2435, 2007.
15. van Andel, C.J., Pistecky, P.V., and Borst, C. Mechanical properties of porcine and human arteries: implications for coronary anastomotic connectors. Ann Thorac Surg **76,** 58, 2003.
16. L'Heureux, N., McAllister, T.N., and de la Fuente, L.M. Tissue-engineered blood vessel for adult arterial revascularization. N Engl J Med **357,** 1451, 2007.
17. Dahl, S.L., Rhim, C., Song, Y.C., and Niklason, L.E. Mechanical properties and compositions of tissue engineered and native arteries. Ann Biomed Eng **35,** 348, 2007.
18. Dahl, S.L., Vaughn, M.E., and Niklason, L.E. An ultrastructural analysis of collagen in tissue engineered arteries. Ann Biomed Eng **35,** 1749, 2007.
19. Zhang, W.J., Liu, W., Cui, L., and Cao, Y. Tissue engineering of blood vessel. J Cell Mol Med **11,** 945, 2007.
20. Isenberg, B.C., Williams, C., and Tranquillo, R.T. Small-diameter artificial arteries engineered *in vitro*. Circ Res **98,** 25, 2006.

21. Grenier, G., Remy-Zolghadri, M., Bergeron, F., Guignard, R., Baker, K., Labbe, R., Auger, F.A., and Germain, L. Mechanical loading modulates the differentiation state of vascular smooth muscle cells. Tissue Eng **12,** 3159, 2006.
22. L'Heureux, N., Stoclet, J.C., Auger, F.A., Lagaud, G.J., Germain, L., and Andriantsitohaina, R. A human tissue-engineered vascular media: a new model for pharmacological studies of contractile responses. FASEB J **15,** 515, 2001.
23. Yazdani, S.K., and Christ, G.J. Engineering of large diameter vessels. In: Atala, A., Lanza, R., Thomson, J., and Nerem, R., eds. Principles of Regenerative Medicine, volume 2007. New York, NY: Academic Press, 2007, pp. 964–986.
24. Stegemann, J.P., Hong, H., and Nerem, R.M. Mechanical, biochemical, and extracellular matrix effects on vascular smooth muscle cell phenotype. J Appl Physiol **98,** 2321, 2005.
25. McFetridge, P.S., Abe, K., Horrocks, M., and Chaudhuri, J.B. Vascular tissue engineering: bioreactor design considerations for extended culture of primary human vascular smooth muscle cells. ASAIO J **53,** 623, 2007.
26. Kaushal, S., Amiel, G.E., Guleserian, K.J., Shapira, O.M., Perry, T., Sutherland, F.W., Rabkin, E., Moran, A.M., Schoen, F.J., Atala, A., Soker, S., Bischoff, J., and Mayer, J.E. Jr. Functional small-diameter neovessels created using endothelial progenitor cells expanded *ex vivo*. Nat Med **7,** 1035, 2001.
27. Yamamoto, M., Yamamoto, K., and Noumura, T. Type I collagen promotes modulation of cultured rabbit arterial smooth muscle cells from a contractile to a synthetic phenotype. Exp Cell Res **204,** 121, 1993.
28. Jacob, M.P., Fulop, T., Jr., Foris, G., and Robert, L. Effect of elastin peptides on ion fluxes in mononuclear cells, fibroblasts, and smooth muscle cells. Proc Natl Acad Sci USA **84,** 995, 1987.
29. Qin, H., Ishiwata, T., Wang, R., Kudo, M., Yokoyama, M., Naito, Z., and Asano, G. Effects of extracellular matrix on phenotype modulation and MAPK transduction of rat aortic smooth muscle cells *in vitro*. Exp Mol Pathol **69,** 79, 2000.
30. Stegemann, J.P., Dey, N.B., Lincoln, T.M., and Nerem, R.M. Genetic modification of smooth muscle cells to control phenotype and function in vascular tissue engineering. Tissue Eng **10,** 189, 2004.
31. Seliktar, D., Black, R.A., Vito, R.P., and Nerem, R.M. Dynamic mechanical conditioning of collagen-gel blood vessel constructs induces remodeling *in vitro*. Ann Biomed Eng **28,** 351, 2000.
32. Buttafoco, L., Engbers-Buijtenhuijs, P., Poot, A.A., Dijkstra, P.J., Vermes, I., and Feijen, J. Physical characterization of vascular grafts cultured in a bioreactor. Biomaterials **27,** 2380, 2006.
33. Butcher, J.T., Barrett, B.C., and Nerem, R.M. Equibiaxial strain stimulates fibroblastic phenotype shift in smooth muscle cells in an engineered tissue model of the aortic wall. Biomaterials **27,** 5252, 2006.
34. Stegemann, J.P., and Nerem, R.M. Altered response of vascular smooth muscle cells to exogenous biochemical stimulation in two- and three-dimensional culture. Exp Cell Res **283,** 146, 2003.
35. Jeong, S.I., Kwon, J.H., Lim, J.I., Cho, S.W., Jung, Y., Sung, W.J., Kim, S.H., Kim, Y.H., Lee, Y.M., Kim, B.S., Choi, C.Y., and Kim, S.J. Mechano-active tissue engineering of vascular smooth muscle using pulsatile perfusion bioreactors and elastic PLCL scaffolds. Biomaterials **26,** 1405, 2005.
36. Riha, G.M., Lin, P.H., Lumsden, A.B., Yao, Q., and Chen, C. Roles of hemodynamic forces in vascular cell differentiation. Ann Biomed Eng **33,** 772, 2005.
37. Lee, S.H., Kim, B.S., Kim, S.H., Choi, S.W., Jeong, S.I., Kwon, I.K., Kang, S.W., Nikolovski, J., Mooney, D.J., Han, Y.K., and Kim, Y.H. Elastic biodegradable poly(glycolide-co-caprolactone) scaffold for tissue engineering. J Biomed Mater Res A **66,** 29, 2003.
38. Park, J.S., Chu, J.S., Cheng, C., Chen, F., Chen, D., and Li, S. Differential effects of equiaxial and uniaxial strain on mesenchymal stem cells. Biotechnol Bioeng **88,** 359, 2004.
39. Nikolovski, J., Kim, B.S., and Mooney, D.J. Cyclic strain inhibits switching of smooth muscle cells to an osteoblast-like phenotype. FASEB J **17,** 455, 2003.
40. Kurpinski, K., Park, J., Thakar, R.G., and Li, S. Regulation of vascular smooth muscle cells and mesenchymal stem cells by mechanical strain. Mol Cell Biomech **3,** 21, 2006.
41. Hamilton, D.W., Maul, T.M., and Vorp, D.A. Characterization of the response of bone marrow-derived progenitor cells to cyclic strain: implications for vascular tissue-engineering applications. Tissue Eng **10,** 361, 2004.
42. Cha, J.M., Park, S.N., Noh, S.H., and Suh, H. Time-dependent modulation of alignment and differentiation of smooth muscle cells seeded on a porous substrate undergoing cyclic mechanical strain. Artif Organs **30,** 250, 2006.
43. Gupta, V., and Grande-Allen, K.J. Effects of static and cyclic loading in regulating extracellular matrix synthesis by cardiovascular cells. Cardiovasc Res **72,** 375, 2006.
44. Li, L., Couse, T.L., Deleon, H., Xu, C.P., Wilcox, J.N., and Chaikof, E.L. Regulation of syndecan-4 expression with mechanical stress during the development of angioplasty-induced intimal thickening. J Vasc Surg **36,** 361, 2002.
45. Merrilees, M.J., Merrilees, M.A., Birnbaum, P.S., Scott, P.J., and Flint, M.H. The effect of centrifugal force on glycosaminoglycan production by aortic smooth muscle cells in culture. Atherosclerosis **27,** 259, 1977.
46. Hamada, M., Kusuyama, Y., Nishio, I., Ura, M., Takeda, J., Hano, T., and Masuyama, Y. Effect of centrifugal force and catecholamines on glycosaminoglycans synthesis of vascular smooth muscle cells in culture. Atherosclerosis **83,** 147, 1990.
47. Hein, M., Fischer, J., Kim, D.K., Hein, L., and Pratt, R.E. Vascular smooth muscle cell phenotype influences glycosaminoglycan composition and growth effects of extracellular matrix. J Vasc Res **33,** 433, 1996.
48. O'Callaghan, C.J., and Williams, B. Mechanical strain-induced extracellular matrix production by human vascular smooth muscle cells: role of TGF-beta(1). Hypertension **36,** 319, 2000.
49. Ma, Y.H., Ling, S., and Ives, H.E. Mechanical strain increases PDGF-B and PDGF beta receptor expression in vascular smooth muscle cells. Biochem Biophys Res Commun **265,** 606, 1999.
50. Smith, J.D., Davies, N., Willis, A.I., Sumpio, B.E., and Zilla, P. Cyclic stretch induces the expression of vascular endothelial growth factor in vascular smooth muscle cells. Endothelium **8,** 41, 2001.
51. Nykanen, A.I., Krebs, R., Tikkanen, J.M., Raisky, O., Sihvola, R., Wood, J., Koskinen, P.K., and Lemstrom, K.B. Combined vascular endothelial growth factor and platelet-derived growth factor inhibition in rat cardiac allografts: beneficial

effects on inflammation and smooth muscle cell proliferation. Transplantation **79,** 182, 2005.
52. Li, S., Lao, J., Chen, B.P., Li, Y.S., Zhao, Y., Chu, J., Chen, K.D., Tsou, T.C., Peck, K., and Chien, S. Genomic analysis of smooth muscle cells in 3-dimensional collagen matrix. FASEB J **17,** 97, 2003.
53. Grassl, E.D., Oegema, T.R., and Tranquillo, R.T. A fibrin-based arterial media equivalent. J Biomed Mater Res A **66,** 550, 2003.
54. Rocnik, E.F., Chan, B.M., and Pickering, J.G. Evidence for a role of collagen synthesis in arterial smooth muscle cell migration. J Clin Invest **101,** 1889, 1998.

Address reprint requests to:
George J. Christ, Ph.D.
Wake Forest Institute for Regenerative Medicine
Wake Forest University School of Medicine
Medical Center Blvd.
Winston-Salem, NC 27157

E-mail: gchrist@wfubmc.edu

Received: February 6, 2008
Accepted: November 18, 2008
Online Publication Date: March 13, 2009